A&A 443, 337–345 (2005)
DOI: 10.1051/0004-6361:20052938

Astronomy & Astrophysics

Extrasolar planets and brown dwarfs around A-F type stars⋆

I. Performances of radial velocity measurements, first analyses of variations

F. Galland[1,2], A.-M. Lagrange[1], S. Udry[2], A. Chelli[1], F. Pepe[2], D. Queloz[2], J.-L. Beuzit[1], and M. Mayor[2]

[1] Laboratoire d'Astrophysique de l'Observatoire de Grenoble, Université Joseph Fourier, BP 53, 38041 Grenoble, France
e-mail: Franck.Galland@obs.ujf-grenoble.fr
[2] Observatoire de Genève, 51 Ch. des Maillettes, 1290 Sauverny, Switzerland

Received 25 February 2005 / Accepted 23 August 2005

ABSTRACT

We present the performances of a radial velocity measurement method that we developed for A-F type stars. These perfomances are evaluated through an extensive set of simulations, together with actual radial velocity observations of such stars using the ELODIE and HARPS spectrographs. We report the case of stars constant in radial velocity, the example of a binary detection on HD 48097 (an A2V star, with $v \sin i$ equal to 90 km s^{-1}) and a confirmation of the existence of a 3.9 $M_{\rm Jup}$ planet orbiting around HD 120136 (Tau Boo). The instability strip problem is also discussed. We show that with this method, it is in principle possible to detect planets and brown dwarfs around A-F type stars, thus allowing further study of the impact of stellar masses on planetary system formation over a wider range of stellar masses than is currently done.

Key words. techniques: radial velocities – stars: binaries: spectroscopic – stars: low-mass, brown dwarfs – stars: planetary systems

1. Introduction

Since the discovery of the first exoplanet around a solar-like star a decade ago (Mayor & Queloz 1995), more than 150 planets have been found by radial velocity surveys[1]. These surveys focus on late type stars (≳F8) as these stars exhibit numerous lines with low rotational broadening. General characteristics of planet masses, distances to star, eccentricities (see e.g. Udry et al. 2003b; Marcy et al. 2003), as well as characteristics of the stars hosting those giant planets (e.g. metallicity; Santos et al. 2003) were derived and allow theoreticians to constrain planetary system formation and evolution (e.g. planet migration) around solar type stars.

A general and fundamental question concerning planet formation is the impact of the mass of the central star on the formation and evolution process. We know that the disks around these different types of stars do not have the same properties at similar ages: T Tauri disks of a few Myr appear to be less evolved than those around massive stars also of a few Myr such as HD 141569 or HR 4796; this tends to show that these disks, as the parent stars, evolve more rapidly (Lagrange et al. 2004). The occurrence and time scale of planet formation have to be investigated and compared.

Looking for planets around early type stars is a difficult task. So far, the studies have been limited to giant stars (Sato et al. 2003; Lovis et al. 2005). These stars have small rotational velocities, but a large radius resulting in minimum possible orbital periods of the order of 100 days or slightly less. In a complementary way, to focus on main sequence stars allows us to access smaller orbital periods and to address the question of evolutionary time scale. These high-mass main sequence stars have not been investigated so far as they exhibit fewer lines that are generally broadened by high rotational velocities (typically 100–200 km s^{-1} for A-type stars; see Fig. 1). It was then thought that the radial velocity method could not be applied to those objects. Indeed, the method to process the data and extract the Doppler information for low-mass stars with the cross-correlation method, is not straightforwardly applicable to more massive stars (Griffin et al. 2000).

A new method for radial velocity measurements was introduced a few years ago (Chelli 2000). It consists of correlating, in Fourier space, each spectrum of the target star and a reference spectrum specific to that star (built e.g. by summing all the available spectra of the star). This method had been applied to solar-type stars; we have adapted it for earlier type stars (Sect. 2). We then performed radial velocity observations

⋆ Based on observations made with the ELODIE spectrograph at the Observatoire de Haute-Provence (CNRS, France) and with the HARPS spectrograph at La Silla Observatory (ESO, Chile) under program ID 073.C-0733.

[1] A list of discovered planets updated by Jean Schneider is available at http://www.obspm.fr/encycl/cat1.html

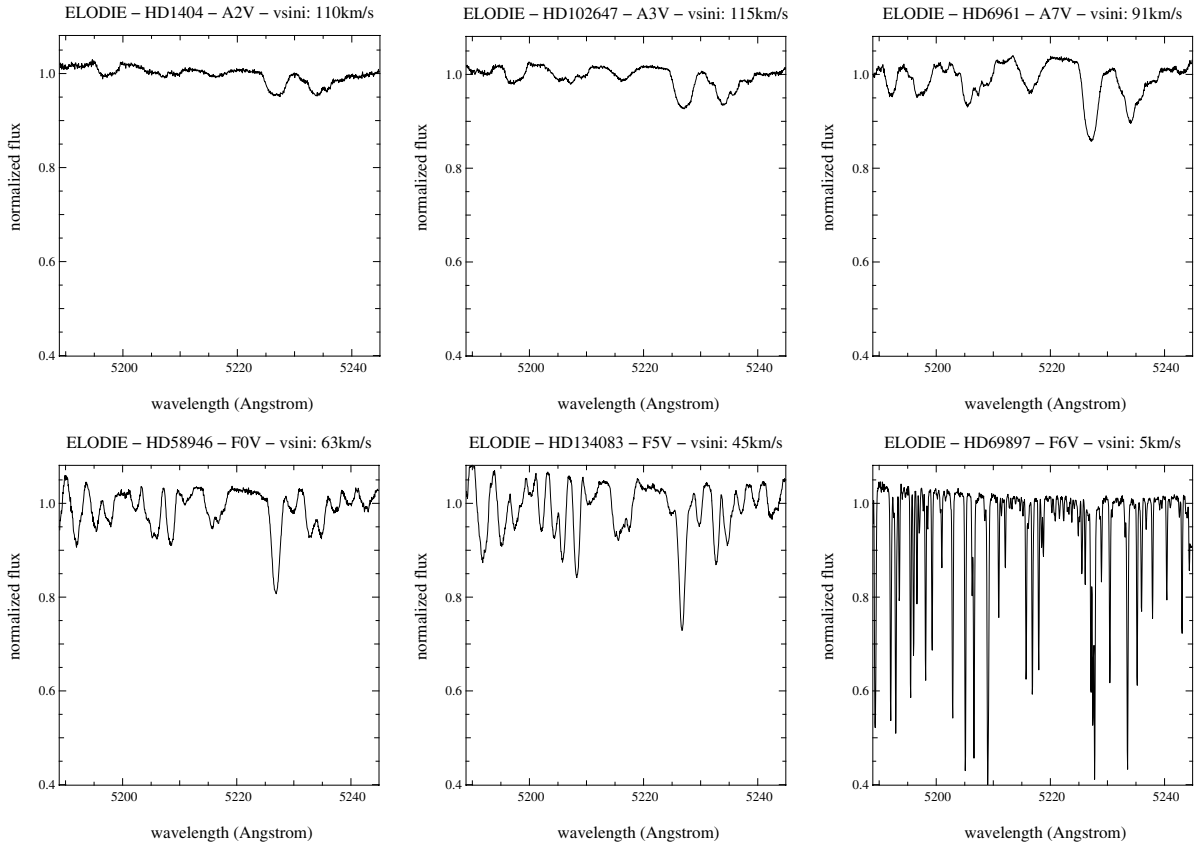

Fig. 1. Examples of spectra acquired with ELODIE. Note the effect of the spectral type and $v \sin i$ on the number, depth and width of the lines.

of A-F type stars, using the fiber-fed echelle spectrographs ELODIE (Baranne et al. 1996), mounted on the 1.93-m telescope at the Observatoire de Haute Provence (CNRS, France) in the northern hemisphere, and HARPS (Pepe et al. 2002), recently installed on the 3.6-m ESO telescope at La Silla Observatory (ESO, Chile) in the southern hemisphere.

We present here the performances obtained by applying this method to these spectroscopic observations of A–F main sequence stars. We demonstrate in particular that it should be possible to detect planets and brown dwarfs around A–F type stars. Results obtained with simulations are provided in Sect. 3. We confirm in Sect. 4 the accuracy of the computed radial velocities and corresponding uncertainties in real cases, with examples of stars constant in radial velocity, the case of a binary detection and the confirmation of a 3.9 $M_{\rm Jup}$ planet orbiting around HD 120136 (Tau Boo). Furthermore, we discuss the first trends observed in radial velocity variations as a function of the spectral type in the range [A0–F7]. Finally, we present the uncertainties achieved for all stars already observed (Sect. 5), and the corresponding mass detection limits in the frame of planet and brown dwarf searches (Sect. 6).

2. Principle of the method

To compute the radial velocity, we use the method described in Chelli (2000). Considering a reference spectrum $S_r(\lambda)$ and a Doppler shifted one, $S(\lambda) = S_r(\lambda - \lambda\frac{U}{c})$, where U is the radial velocity associated with $S(\lambda)$, we derive the cross spectrum:

$$\widehat{I}(\nu) = \widehat{S}_r(\nu)\widehat{S}^*(\nu) = \mathrm{e}^{2\mathrm{i}\pi\nu\lambda_0\frac{U}{c}}|\widehat{S}_r(\nu)|^2.$$

The radial velocity is contained in the phase of $\widehat{I}(\nu)$. We then look for the velocity V which minimizes in a least square sense the imaginary part of the quantity: $\widehat{C}(\nu) = \mathrm{e}^{-2\mathrm{i}\pi\nu\lambda_0\frac{V}{c}}\widehat{I}(\nu)$. The quantity to be minimized becomes:

$$\chi^2 = \sum_j \frac{\mathrm{Im}^2[\widehat{C}(\nu_j)]}{\sigma^2(\nu_j)} = \sum_j \frac{\sin^2(2\mathrm{i}\pi\nu_j\lambda_0\frac{U-V}{c})|\widehat{S}_r(\nu)|^4}{\sigma^2(\nu_j)}$$

which is minimum when V reaches the radial velocity shift U. ν_j are discrete frequencies. The photonic radial velocity uncertainty ($\epsilon_{RV-\mathrm{Ph}}$) is simultaneously calculated using the photon noise statistic. See Chelli (2000) for further details.

Working in the Fourier space allows us to apply frequency cuts, reducing the impact of the noise (high frequencies) and of the variations of the continuum (low frequencies) due to stellar phenomena or instrumental effects. This is particularly interesting in the case of A–F type stars.

3. Radial velocity measurements and uncertainties estimates: simulations

We first present simulations performed to test our radial velocity and photon noise uncertainty ($\epsilon_{RV-\mathrm{Ph}}$) determination on individual measurements.

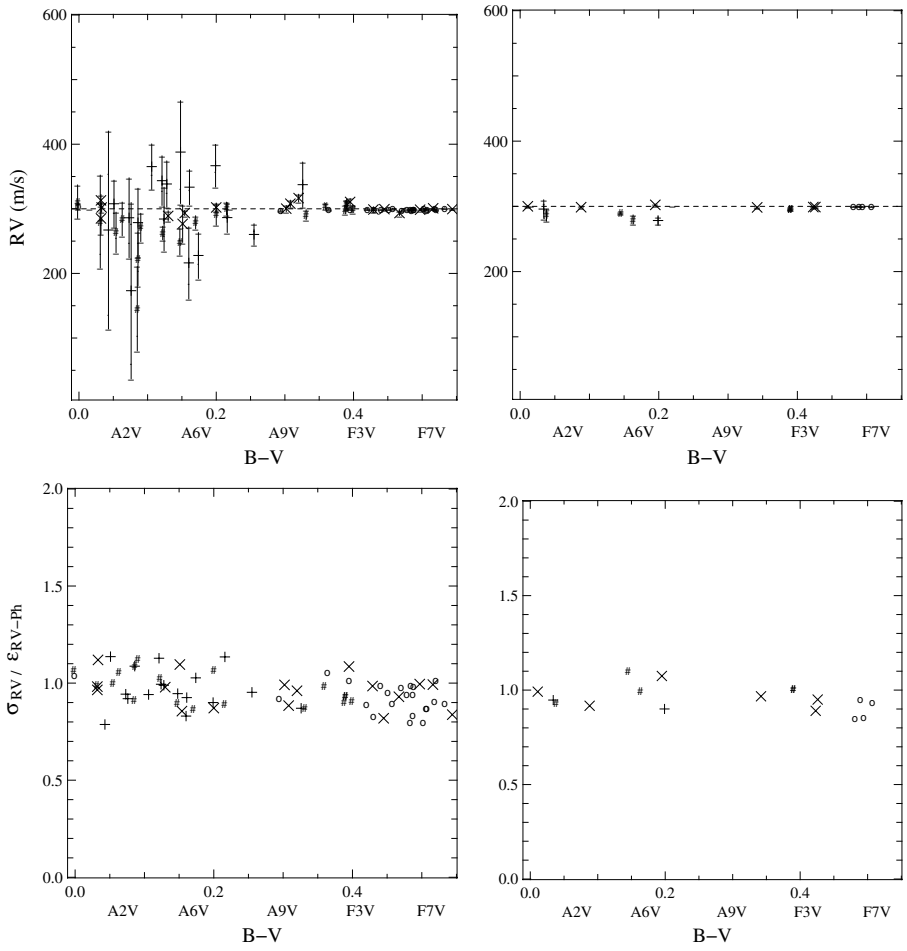

Fig. 2. *Top*: average computed radial velocity obtained by simulations on spectra acquired with ELODIE (*left*) and HARPS (*right*). Error bars from the average of 100 test spectra. *Bottom*: radial velocity dispersions divided by uncertainties obtained from simulations on ELODIE (*left*) and HARPS (*right*) spectra. Conventions for symbols: $v \sin i \leq 20$ km s^{-1} (o), 20 km s^{-1} $\leq v \sin i \leq 70$ km s^{-1} (×), 70 km s^{-1} $\leq v \sin i \leq 130$ km s^{-1} (#), 130 km s^{-1} $\leq v \sin i$ (+).

3.1. Test spectra

We consider here the case of identical spectra shifted with a constant radial velocity. We first consider a spectrum of a given star obtained with ELODIE or HARPS; this spectrum is smoothed then duplicated into several spectra (here, 101). We add noise to one of these spectra at a level corresponding to a typical reference spectrum, namely corresponding to the sum of 100 spectra with *S/N* equal to 200 in the case of ELODIE, and 400 in the case of HARPS. We add noise to the other 100 spectra at a level corresponding to a typical measurement i.e. $S/N = 200$ with ELODIE and 400 with HARPS. Then, these spectra are shifted in radial velocity with a given value (here, 300 m s^{-1}), typically induced by the presence of a planet.

Our method is then used to measure the radial velocities and the corresponding uncertainties. For the considered star, we obtain a distribution of computed radial velocities, characterized with its average and dispersion (if assumed gaussian). The advantages of these tests are: the original spectrum corresponds to a real case in terms of number and depth of spectral lines, taking into account rotational broadening and spectral type which are key parameters; the average radial velocity measured can be compared to the shift applied, in order to test the radial velocity measurement process; no effect other than velocity shift changes the spectra.

3.2. Results

The radial velocity measurements obtained are shown in Fig. 2 (top), for different spectral types (ranging between A0V and F7V), and different rotational velocities ($v \sin i$). The measurements correspond to the average on the distribution of computed radial velocities for a given star. Error bars correspond to $\frac{\epsilon_{RV-\mathrm{Ph}}}{\sqrt{100}} = \epsilon'_{RV-\mathrm{Ph}}$, as they correspond to the 100 test spectra for a given star. The average computed radial velocity is consistent with the initial shift RV_0 equal to 300 m s^{-1}, given the error bars. This demonstrates the accuracy of the computed radial velocities (no systematic error), in the case of identical spectra only shifted in radial velocity.

The associated uncertainties are shown in Fig. 2. In all cases, the radial velocity dispersion σ_{RV} on the radial velocity distribution obtained for each star is consistent with the computed uncertainties $\epsilon_{RV-\mathrm{Ph}}$: the distribution of $\frac{\sigma_{RV}}{\epsilon_{RV-\mathrm{Ph}}}$ on the results obtained for the different stars is centered on 0.95 ± 0.09

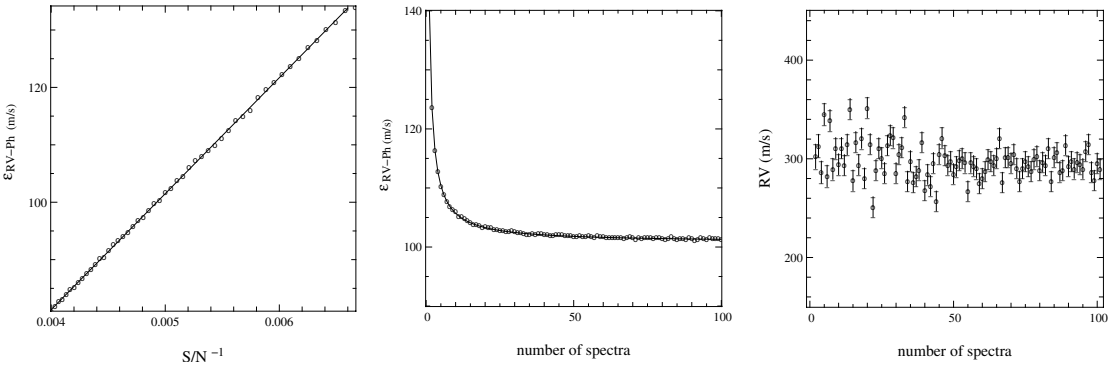

Fig. 3. Simulated radial velocity uncertainties versus *S/N* (*left*), versus the number of spectra used to build the reference spectrum (*center*), and radial velocities obtained as a function of this number of spectra (*right*), in the case of an A7V star, $v \sin i = 90$ km s^{-1}, with ELODIE.

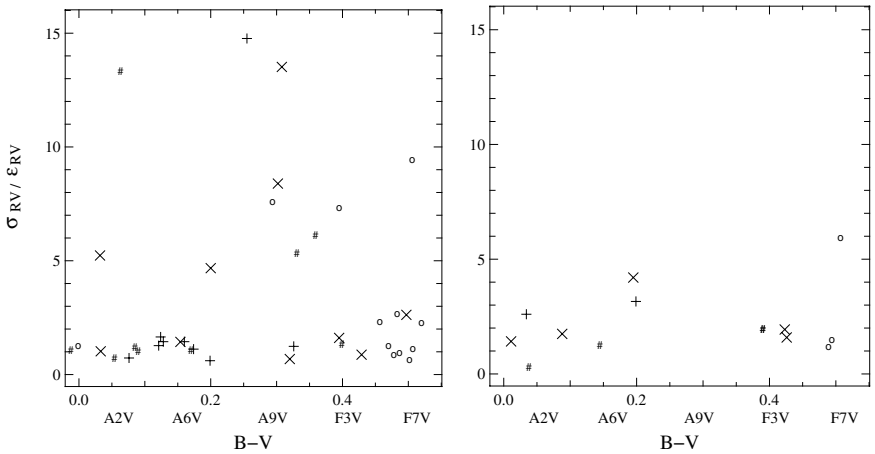

Fig. 4. Measured dispersions divided by uncertainties obtained with ELODIE (*left*) and HARPS (*right*), with at least 5 measurements. *S/N* are those obtained during observations. Symbols are the same as in Fig. 2.

for ELODIE, and on 0.94 ± 0.1 for HARPS. This demonstrates the quality of the photon noise uncertainty estimates.

The same kind of tests as above (creation of 100 test spectra shifted by 300 m s^{-1}, and a reference spectrum) have been performed to check the dependence of $\epsilon_{RV-\mathrm{Ph}}$ on the number n of spectra used to compute the reference spectrum (with S/N fixed to 200) and on S/N (with n fixed to 100). We find that the radial velocity uncertainties behave following these relations: $\epsilon_{RV-\mathrm{Ph}} \propto \frac{1}{S/N}$ where *S/N* is the signal–to–noise per pixel for one spectrum. This is useful when planning measurements, regarding the exposure time necessary to reach a given $\epsilon_{RV-\mathrm{Ph}}$; $\epsilon_{RV-\mathrm{Ph}} \propto \sqrt{\frac{n+1}{n}}$ is nearly constant for $n \geq 10$.

The results of the computation are displayed in Fig. 3 as dots: they are in good agreement with fits corresponding to these relations. Moreover, the radial velocities are not affected by systematic errors, even if the number of spectra used to build the reference spectrum is small (Fig. 3).

4. Radial velocity dispersions and uncertainties: real case

Our aim is to confirm the accuracy of the computed radial velocities and corresponding uncertainties in real cases. We use here the data available so far on our sample of stars surveyed with ELODIE and HARPS. By January 2005, 45 A–F type stars were observed at least 5 times with ELODIE (S/N equal to 196 on average) and 13 with HARPS (S/N equal to 302 on average).

The dispersions obtained, compared to the observed radial velocity uncertainties, are displayed in Fig. 4. They are consistent with an accurate computation of the radial velocity uncertainties in real cases, because they verify $\sigma_{RV} \gtrsim \epsilon_{RV}$ in most cases, where $\epsilon_{RV} = \sqrt{\epsilon^2_{RV-\mathrm{Ph}} + \epsilon^2_{RV-\mathrm{Ins}}}$. In addition to the photon noise, ϵ_{RV} takes into account instrumental (in)stability ($\epsilon_{RV-\mathrm{Ins}}$: 6.5 m s^{-1} with ELODIE, 1 m s^{-1} with HARPS).

Radial velocity uncertainties observed and simulated (normalized to the same *S/N*) are in good agreement (see Fig. 6): in most cases, differences are smaller than 20%. Uncertainties observed seem slightly larger than the ones simulated, except for stars with $B - V \geq 0.4$ and $v \sin i \leq 20$ km s^{-1}: spectra may be different from one to the other in real cases, resulting in imperfections in the reference spectrum, hence larger uncertainties; these imperfections could be negligible for late type stars, given the large number and depth of the lines.

4.1. Stars constant in radial velocity

Examples of radial velocity measurements obtained with ELODIE for stars that appear to be constant in radial velocity (given our temporal spans) are displayed in Fig. 5, and the corresponding dispersions and uncertainties are given in Table 1.

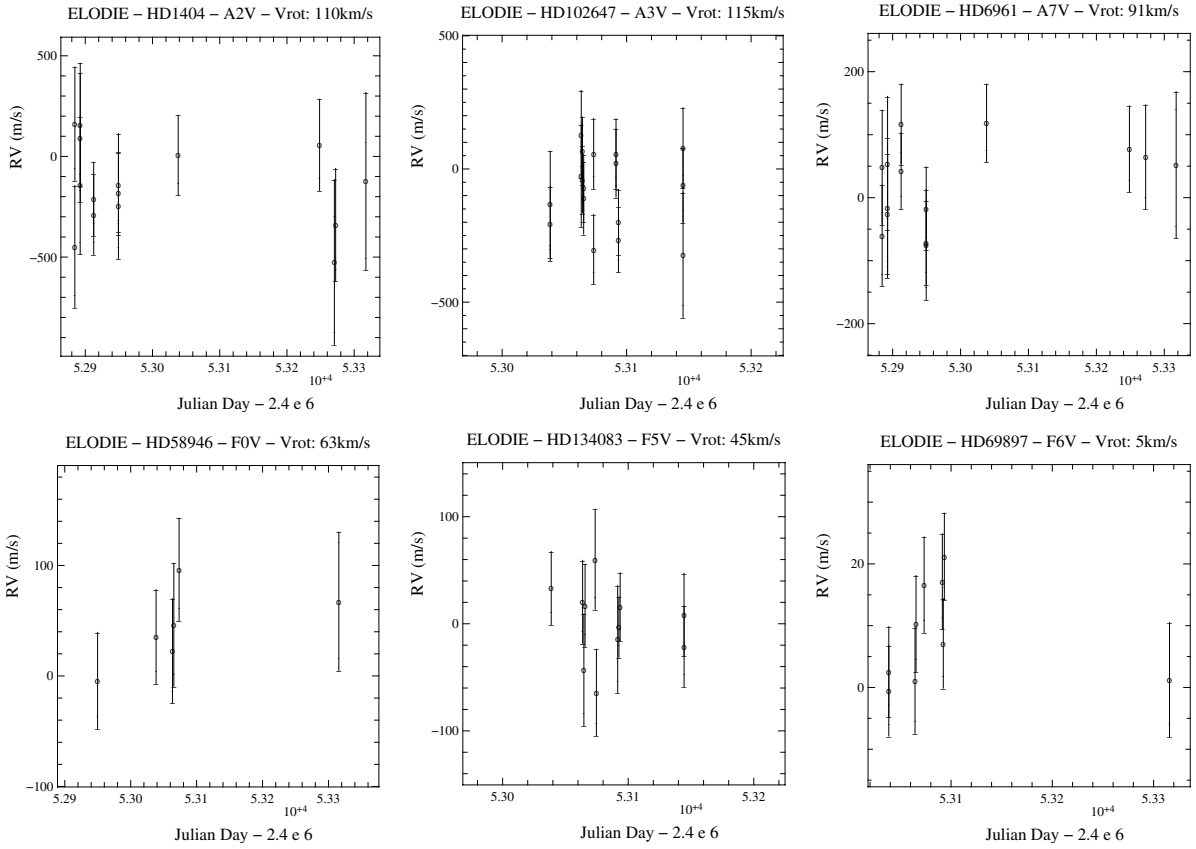

Fig. 5. Examples of radial velocity measurements obtained in the case of stars constant in radial velocity, given the present error bars.

Table 1. Radial velocity (*RV*) dispersion and uncertainties (measured and normalized to the same *S/N*, 200) for a set of stars observed with ELODIE and constant in radial velocity. The normalization allows us to focus the comparison between stars only on spectral type and $v \sin i$.

Star	spectral type	$v \sin(i)$ km s^{-1}	Number of measurements	Dispersion on measured *RV* (m s^{-1})	Measured *RV* uncertainties (m s^{-1})	Normalized *RV* uncertainties (m s^{-1})
HD 1404	A2V	110	15	203	280	318
HD 102647	A3V	115	17	137	132	222
HD 6961	A7V	91	15	88	83	104
HD 58946	F0V	63	6	32	47	66
HD 134083	F5V	45	11	34	39	44
HD 69897	F6V	5	9	7.7	7.7	7.4

The radial velocity dispersions are consistent with the uncertainties: this confirms the quality of the estimation of the later.

4.2. HD48097: a binary system

Among stars variable in our radial velocity measurements, we report here a binary detection in HD 48097 (HIP 32104), an A2V, $v \sin i = 90$ km s^{-1} star, with $B - V = 0.063$, $V = 5.21$, located at 43 pc from the Sun. The orbital parameters deduced from a Keplerian adjustment (Fig. 7) are displayed in Table 2. The companion is a star with a mimimum mass of 0.43 $M_\odot$, thus a late K or M type dwarf (and not a white dwarf for example, which should have evolved faster than the primary, whose mass is 2.7 $M_\odot$). The dispersion of the residuals is 192 m s^{-1} rms, consistent with the radial velocity uncertainties (359 m s^{-1} on average, 283 m s^{-1} if normalized to $S/N = 200$); the difference can be due to the small number of available measurements. This confirms the accuracy of the computed radial velocities in a real case.

4.3. HD 120136: Tau Boo, a known planet

As another example, we show the measurements obtained on Tau Boo (HD 120136, HR 5185), an F7V star, with $B - V = 0.48$, $V = 4.50$, located 15 pc from the Sun. We confirm the existence of a planet orbiting around this star (Butler et al. 1997). The orbital parameters (Fig. 8) deduced from a Keplerian adjustment are displayed in Table 2, fixing e and ω to 0 given the small number of measurements. They are consistent with the values $P = 3.3128 \pm 0.0002$ days, $e = 0.02 \pm 0.02$, $K_1 = 469 \pm 5$ m s^{-1} previously found. Assuming a primary mass of 1.2 $M_\odot$, the minimum mass of the companion is still 3.9 $M_{\rm Jup}$ with a semimajor axis of 0.046 AU.

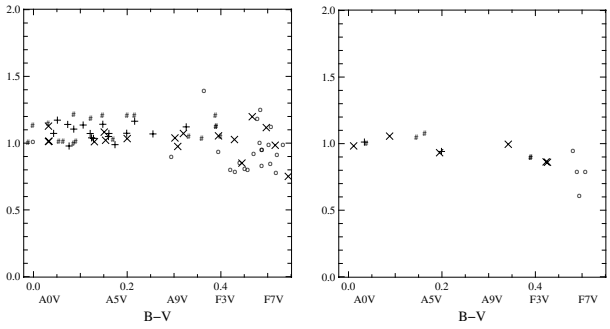

Fig. 6. Radial velocity uncertainties obtained in real cases ($\epsilon_{RV\mathrm{real}}$) divided by simulated radial velocity uncertainties ($\epsilon_{RV\mathrm{simulated}}$), with ELODIE (*left*) and HARPS (*right*). Symbols are the same as in Fig. 2.

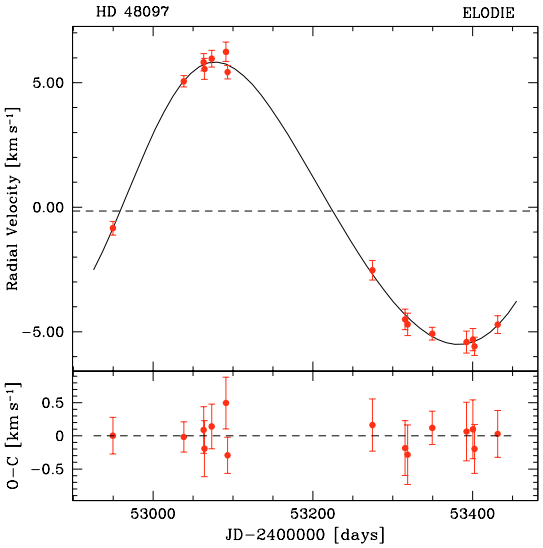

Fig. 7. ELODIE radial velocity data and orbital solutions for HD 48097. *Top*: radial velocities. *Bottom*: residuals.

Table 2. ELODIE orbital solution for HD48097 and Tau Boo.

Parameter		HD 48097	Tau Boo
P	[days]	552 ± 17	3.3135 ± 0.0014
T	[JD-2 450 000]	3005 ± 40	1.27 ± 0.03
e		0.10 ± 0.03	0 (fixed)
γ	[km s^{-1}]	-0.16 ± 0.23	-0.0650 ± 0.004
ω	[deg]	304 ± 29	0 (fixed)
K	[km s^{-1}]	5.67 ± 0.11	0.476 ± 0.005
N_{meas}		15	7
σ(O−C)	[km s^{-1}]	0.19	0.014
$a_1 \sin i$	[AU]	0.286	1.5×10^{-4}
$f(m)$	[$M_\odot$]	1.03×10^{-2}	3.7×10^{-8}
m_1	[$M_\odot$]	2.7	1.2
$m_2 \sin i$	[M_{Jup}]	430	3.9
a	[AU]	1.9	0.046

This also confirms the accuracy of the computed radial velocities, in the case of a spectral type sufficiently late to have been already explored. A detection of a planet orbiting an F6V star can be found in Galland et al. (2005b).

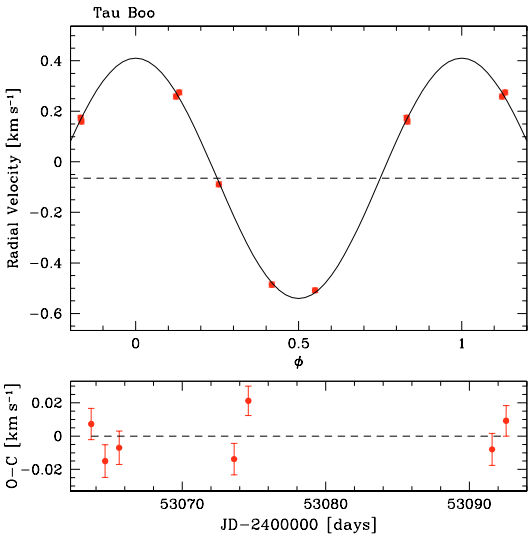

Fig. 8. ELODIE radial velocity data and orbital solutions for Tau Boo. *Top*: phased-folded velocities. *Bottom*: residuals.

4.4. Instability strip

It appears (Fig. 4) that the late A and early F type stars observed ($B - V$ between 0.2 and 0.4) are often highly variable in radial velocity. This range of $B - V$ actually corresponds to the intersection of the instability strip and the main sequence, where we find the pulsating δ Scuti (Handler et al. 2002; Breger et al. 2000) and γ Dor stars (Mathias et al. 2004; Handler et al. 2002). These stars can be responsible for radial velocity variations with an amplitude up to several km s^{-1} and periods up to several days. Additional observations are needed to check for each of the stars observed with $B - V$ in the range 0.2–0.4 and with high radial velocity variations if they are members of the δ Scuti and γ Dor groups.

The studies on the associated photometric variations (Eyer et al. 1997) show that the amplitude of these variations can reach 8 mmag with periods of 2 days in this range of spectral types. Yet, the amplitude is less than 2 mmag for the other A–F type stars. The latter may thus be preferential targets if pulsations are not desired to pollute other radial velocity variations.

In particular, it is probable that finding planets with the radial velocity method will be more difficult for stars with $B-V$ in the range 0.2–0.4; ways to distinguish a planetary signal from that of pulsations have to be investigated.

5. Achieved uncertainties: influence of stellar properties

As radial velocity uncertainties have been demonstrated to be accurately computed, we can discuss their values. We consider here the simulated radial velocity uncertainties, as they correspond to the case of identical spectra only shifted in radial velocity (keeping in mind that they are in good agreement with the real case, differences being less than 20% in most cases).

These radial velocity uncertainties are displayed in Fig. 9. We can see that they depend on the spectral type of the star (the later the spectral type, the smaller ϵ_{RV}, for a given range

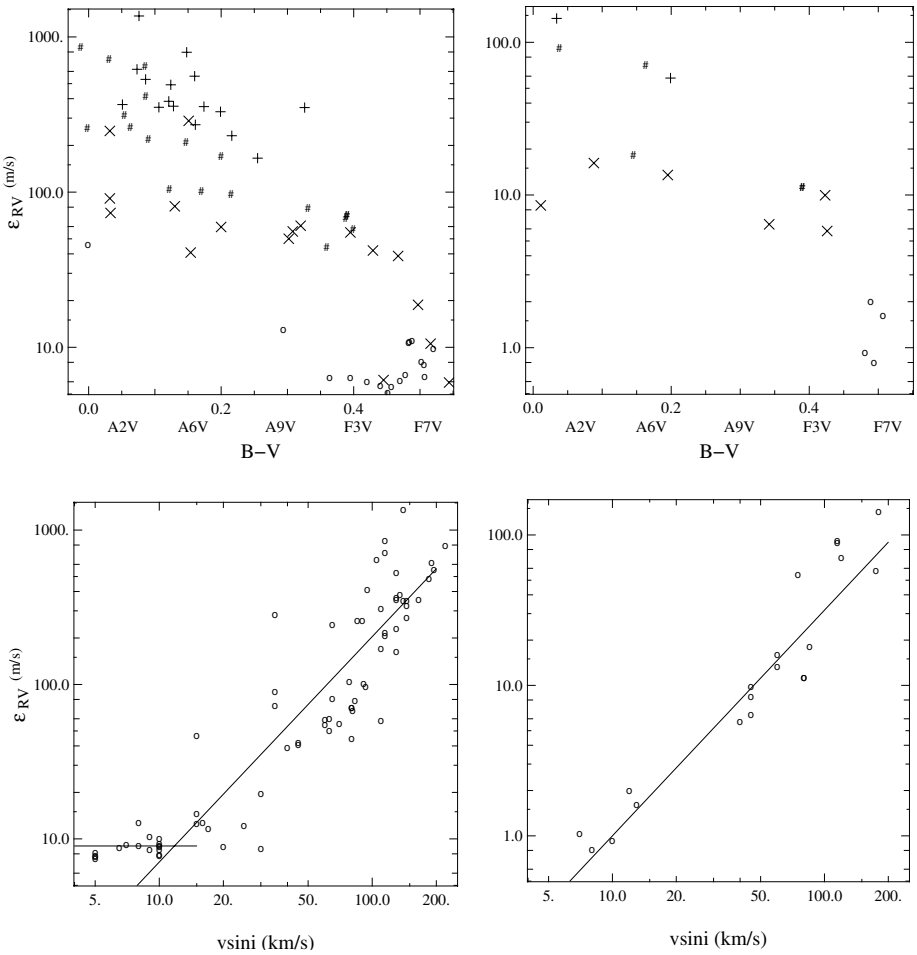

Fig. 9. Uncertainties on the radial velocities in the case of identical spectra only shifted in radial velocity, for all the observed stars, versus $B-V$ (*top*; symbols are the same as in Fig. 2) and $v \sin i$ (*bottom*). The spectra were acquired with ELODIE (*left*) and HARPS (*right*).

of $v \sin i$), and on its rotational velocity to a higher extent. A linear fit of the logarithm of the radial velocity uncertainty (in $\mathrm{m\,s^{-1}}$) as a function of the logarithm of $v \sin i$ (in $\mathrm{km\,s^{-1}}$) gives:

- $\epsilon_{RV} = 0.16 \times v \sin i^{1.54} \times \frac{200}{S/N}$ with ELODIE,
- $\epsilon_{RV} = 0.032 \times v \sin i^{1.50} \times \frac{400}{S/N}$ with HARPS.

The dependance of ϵ_{RV} on $v \sin i$ to the power 1.5, found with these fits, is consistent with the study of Bouchy et al. (2001) on the fundamental photon noise limit to radial velocity measurements, in the case of early F type main sequence stars. These fits apply only in the range where lines are resolved, and if photon noise uncertainties are large compared to the instrumental (in)stability (this corresponds typically to $v \sin i \geq 15$ $\mathrm{km\,s^{-1}}$ with ELODIE). When the lines are not resolved (small $v \sin i$), we reach the instrumental limit, represented by a horizontal line in Fig. 9, in the case of ELODIE. Note that the dispersion around the fits results from stars with different spectral types.

The achieved uncertainties on the radial velocities appear to be a factor of 5 ± 1 lower with spectra obtained with HARPS than with ELODIE, even for early type stars which have on average a large $v \sin i$. A factor of 2 comes from the *S/N* per pixel corresponding to these radial velocity uncertainties (200 with ELODIE versus 400 with HARPS). Another factor of 2 comes from an increased factor of 4 in the number of pixels per spectral element, i.e. a factor of 4 in the whole flux for a given *S/N* per pixel (ELODIE and HARPS have approximatively the same spectral range). For the radial velocity uncertainty, these two effects give a factor of $2 \times 2 = 4$, consistent with the factor 5 ± 1 above.

Note that we reach ELODIE and HARPS instrumental precision for slowly rotating stars.

6. Mass detection limits

In the framework of searches for low mass companions, we now estimate what kind of such companions can be found given these uncertainties.

The mass detection limits are inferred for different orbital periods, given radial velocity variations of $\pm 3\,\epsilon_{RV}$, assuming a circular orbit. They are displayed in Fig. 10. The most important outcomes are:

– With ELODIE, the planetary domain can be reached for A type main sequence stars with $v \sin i$ up to 100 $\mathrm{km\,s^{-1}}$ and orbital periods less than 10 days, or with $v \sin i$ up to 40 $\mathrm{km\,s^{-1}}$ and orbital periods less than 1000 days. For late

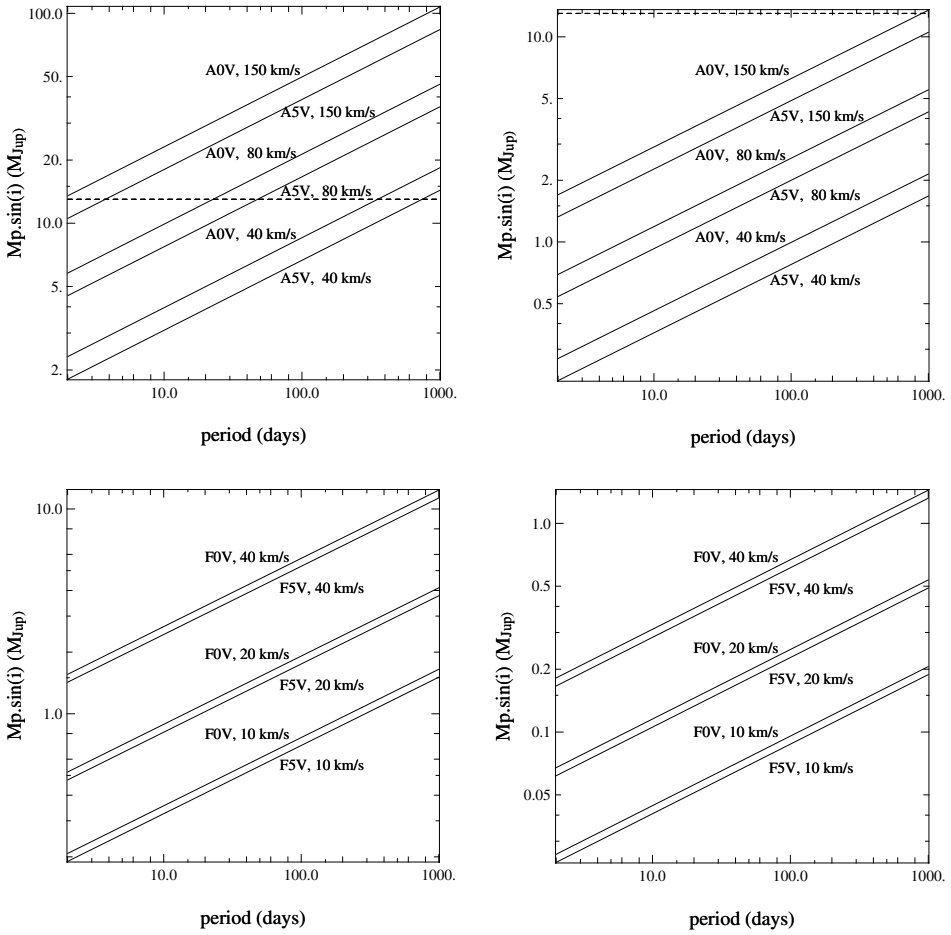

Fig. 10. Mass detection limits for A (*top*) and F (*bottom*) type stars, using ELODIE (*left*) or HARPS (*right*).

A type stars, the accessible range is $v \sin i$ up to 80 km s^{-1} and orbital periods up to 100 days. Planetary masses can be detected for all F type main sequence stars.

– With HARPS, the planetary domain is accessible for all A and F type stars, even with large $v \sin i$.

For example, with ELODIE, the mass detection limit of a 10 d period planet around an A5V star with $v \sin i$ equal to 60 km s^{-1} is 4 $M_{\rm Jup}$. Such massive close-in planets are not unexpected if a proto-planetary massive disk scales with the parent star mass. With HARPS, this detection limit decreases to 0.7 $M_{\rm Jup}$.

7. Conclusions

We presented in this paper the performances of a radial velocity measurement method that we developed in the case of A–F type stars. Radial velocities and corresponding uncertainties are shown to be accurately computed both by simulations and using real cases (stars constant in radial velocity, the case of a binary detection and the confirmation of a known planet orbiting Tau Boo).

With regard to stellar properties, the achieved uncertainties ϵ_{RV} depend on the spectral type, and above all on $v \sin i$, to the power 3/2: if ϵ_{RV} is expressed in m s^{-1} and $v \sin i$ in km s^{-1}, ϵ_{RV} behaves typically (still with a dependance on the spectral type) as:

- $\epsilon_{RV} = 0.2 \times v \sin i^{1.5} \times \frac{200}{S/N}$ with ELODIE, if $v \sin i \geq 15$ km s^{-1};
- $\epsilon_{RV} = 0.03 \times v \sin i^{1.5} \times \frac{400}{S/N}$ with HARPS.

In particular, we have demonstrated that it should be possible to detect extrasolar planets and brown dwarfs around such A–F type stars: detection limits arrive at the planetary domain for most of them. Given these results, we have begun a radial velocity survey to search for these low mass companions around a volume-limited sample of A–F main sequence stars, with ELODIE and HARPS.

Acknowledgements. We acknowledge support from the French CNRS. We are grateful to the Observatoire de Haute Provence, the Programme National de Planétologie (INSU), and ESO for the time allocation, and to their technical staff. These results have made use of the SIMBAD database, operated at CDS, Strasbourg, France.

References

Abt, H. 2000, ApJ, 544, 933
Baranne, A., Queloz, D., Mayor, M., et al. 1996, A&A, 119, 373

Breger, M., & Montgomery, M. H. 2000, ASP Conf. Ser., Vol. 210, Delta Scuti an Related stars (San Francisco: ASP)
Bouchy, F., Pepe, F., & Queloz, D. 2001, A&A, 374, 733
Butler, P., Marcy, G., Williams, E., et al. 1997, ApJ, 474, L115
Chelli, A. 2000, A&A, 358, L59
Eyer, L., & Grenon, M. 1997, Hipp. Conf., 467E
Handler, G., Balona, L. A., Shobbrook, R. R., et al. 2002, MNRAS, 333, 262
ESA 1997, The Hipparcos and Tycho Cat, ESA SP-1200
Griffin, R. E. M., David, M., & Verschueren, W. 2000, A&AS, 147, 299
Lagrange, A. M., Backman, D. E., & Artymowicz, P. 2000, in Protostars and Planets IV (Book - Tucson: University of Arizona Press), ed. V. Mannings, A. P. Boss, & S. S. Russell, 639
Lagrange, A. M., & Augereau, J. C. 2004, in Planetary systems and planets in systems, ISSI workshop
Lovis, C., Mayor, M., & Udry, S. 2005, in Proc. 13th Cool Stars Workshop, ESA SP Ser., in press
Marcy, G., et al. 2003, in Scientific Frontiers in Research on Extrasolar Planets, ed. D. Deming, & S. Seager, ASP Conf. Ser., in press
Mathias, P., Le Contel, J.-M., & Chapellier, E. 2004, A&A, 417, 189
Mayor, M., & Queloz, D. 1995, Nature, 378, 355
Mayor, M., et al. 2003, Proc. of the ISSI Workshop on Planetary Systems and Planets in Systems (Kluwer Academic Press), in press
Pepe, F., Mayor, M., Rupprecht, G., et al. 2002, The ESO Messenger, 110, 9
Santos, N. C., Israelian, G., Mayor, et al. 2003, A&A, 398, 363
Sato, B., Ando, H., Kambe, E., et al. 2003, ApJ, 597, L157
Udry, S., Mayor, M., & Queloz, D. 2003a, in Scientific Frontiers in Research on Extrasolar Planets, ed. D. Deming, & S. Seager, ASP Conf. Ser., in press
Udry, S., Mayor, M., & Santos, N. C. 2003b, A&A, 407, 369